

## **GEANT4 SIMULATION OF AN ACCELERATOR HEAD FOR INTENSITY MODULATED RADIOTHERAPY**

**F. Foppiano**

National Cancer Research Institute (IST)  
Largo Rosanna Benzi 10, 16132 Genova - Italy  
franca.foppiano@istge.it.

**B. Mascialino, M.G. Pia and M. Piergentili**

Italian Institute for Nuclear Research (INFN)  
via Dodecaneso 33, 16146 Genova -Italy  
Barbara.Mascialino@ge.infn.it; MariaGrazia.Pia@ge.infn.it; Michela.Piergentili@ge.infn.it

### **ABSTRACT**

We present a Geant4-based application for the simulation of the absorbed dose distribution given by a medical linac used for intensity modulated radiation therapy (IMRT). The linac geometry is accurately described in Monte Carlo code using the accelerator's manufacturer's specifications. The flexible design of this object-oriented system allows for an easy configuration of the geometry of the treatment head for various types of medical accelerators used in clinical practice.

The precision of the software system relies on the application of Geant4 Low Energy Electromagnetic models, extending the treatment of electron and photon interaction down to low energies for precise dosimetry.

The capability of the software to evaluate dose distribution has been verified by comparison with measurements in water phantom; the comparisons were performed for percent depth dose (PDD) and for flatness at 15, 50 and 100 mm depth for various field size, for a 6 MV electron beam. The source-surface distance (SSD) was 100 cm. We show the comparisons between simulation results and experimental measurements.

The code is fully parallelized, allowing to achieve the high statistics Monte Carlo production required fastly. The parallelization scheme adopted allows to run the code transparently either in a local computing farm or with geographically distributed resources, such as a computing GRID.

This software system is released to the public as an open source software system, for the benefit of the scientific community.

*Key Words:* IMRT, Geant4, Radiotherapy

### **1 INTRODUCTION**

The development of advanced techniques in radiotherapy, such as intensity modulation, brings about the need for more sophisticated and precise methods to calculate dose distributions.

In particular, Intensity Modulated Radiation Therapy (IMRT) involves a series of small fields, to obtain a specific treatment, with a complex dose distribution, for an individual patient.

The most commonly treatment planning systems are based on calculation algorithms, that do not account for electron transport; and, therefore, they do not predict the dose accurately in small fields, where lateral electronic equilibrium is not achieved.

The project described in this paper developed a dosimetric system, based on a Monte Carlo method, that calculates accurately the dose distributions for IMRT.

## 2 MATERIALS AND METHODS

### 2.1 Monte Carlo calculation

GEANT4 [1] is an object-oriented toolkit developed to simulate the passage of particles through matter. It contains a large variety of physics models, covering the interactions of electrons, muons, hadrons and ions with matter from 250 eV up to several PeV. For these features and for its versatility, Geant4 applications are developed not only in particle physics, but also in many other fields, where high accuracy and precision of simulations are needed, such as radiation physics, space science and radiotherapy. Specifically for our application, of particular interest is the Low Energy Package [2], developed to extend electromagnetic interaction of particles with matter down to very low energy: 250 eV for electrons and photons.

We developed a Geant4 application, which simulates the linear accelerator's head used at National Cancer Research Institute in Genova for the IMRT.

The components in the simulated linac head were the following: target, primary collimator, vacuum windows, flattening filter, ion chamber, mirror, jaws on the X and Y coordinates, multileaf collimator, with rounded leaf tips, and the phantom. Each pair of jaws can be rotated through an axis that is perpendicular to the beam axis. The user can select the position of each jaw and of every single leaf of the multileaf collimator. The phantom was divided in voxels, in which we collected the energy deposit to calculate the relative dose absorbed. In the case of squared fields the phantom was made of water, in the case of the intensity modulated fields the phantom was made of plexiglass. We have assumed a Gaussian distribution for energy and momentum of the primary electrons.

### 2.2 Experimental measurements

The measurements of both depth dose curves and lateral dose profiles for the squared fields were made using an ion chamber (31002 Semiflex, PTW, Freiburg Germany) with an active volume of  $0.125 \text{ cm}^3$  and a cavity diameter of 0.55 cm. The ion chamber was mounted on a computer controlled scanning system (MP3-System, PTW, Freiburg Germany). The uncertainty of the position accuracy of the scanning system provided by the manufacturer was  $\pm 0.1 \text{ mm}$ . All the measurements were obtained at a source-surface distance (SSD) of 100 cm. The effective point of measurement for the ion chamber was taken to be  $0.60r_{\text{cav}}$ , where  $r_{\text{cav}}$  is the cavity radius of the chamber, consistent with the International Atomic Energy Agency (IAEA) protocol [3]. The estimated total uncertainty of an ionization measurement at one depth was 0.5%, deriving from the positioning repeatability of the ion chamber and short term fluctuations of the chamber, electrometer, air pressure and temperature, during the time frame of one scan. The estimated total uncertainty of a relative dose measurement was taken to be 1.8%; this estimation takes in account the relative uncertainty on the calibration of the dosimeter, on the correction terms for influence quantities, on the beam quality correction, the long term stability of the dosimeter, on the dosimeter reading, the long term stability of user dosimeter and the establishment of reference conditions.

The measurements of absorbed dose in a plane, for the fields obtained with the multileaf collimator, were made using Kodak X-Omat V films and the film dosimetry system RIT113 with the scanner VXR-16 DosimetryPRO.

## 2.3 Normalization and comparison of data

Data concerning the depth-dose curves were normalized to their maximum value. Lateral profiles obtained with experimental measurements were normalized to the dose value on the beam axis, while the ones obtained with the dosimetric system were normalized to the mean value in the flat zone. Moreover in the specific case of the lateral profiles, we rebinned data in the central flat region, with the aim of reducing statistical fluctuations.

Statistical comparisons between experimental measurements and Geant4 simulations have been performed by means of a Goodness-of-Fit statistical toolkit [4], specialized in the comparison of data distributions. Among the ones available in the toolkit, we have selected the Kolmogorov-Smirnov [5] test. In the particular case of lateral dose profiles, we divided both experimental data and Geant4 simulation results in five regions of interest, having a relevance in the medical-physics domain:

- the central flat zone,
- the two high gradient regions,
- the tails,

and we tested the agreement between the two distributions within each of these regions of interest.

For any analysis performed, the confidence level was set to the value 0.05; a p-value higher than 0.05 led to the acceptance of the null hypothesis, stating the equivalence between reference data and Geant4 simulations.

## 3 RESULTS

In all the simulations, we reproduced with the dosimetric system the real experimental set-up, such as the position of the jaws and of every single leaf of the multileaf collimator, the energy of the beam, the source-surface distance and the material of the phantom.

### 3.1 Field 10x10 cm

We start this study from the 10x10 cm field, that is often used as a reference field to calculate relevant dosimetric quantities.

In Figure 1 we show the lateral dose profiles at 50 mm depth for the 10x10 cm field, with the 6 MV beam (SSD=100 cm). Table I shows the quantitative statistical results obtained in each region of interest: the first and the second columns indicate the region of interest under study, in the third column we reported the distance between the two distributions (Kolmogorov-Smirnov test statistics) and in the fourth column we listed the corresponding p-value. In any region considered, the Kolmogorov-Smirnov test pointed out a good agreement between experimental data and Geant4 simulations (p-values > 0.05 in any case).

In Figure 2 we show the lateral dose profiles at 100 mm depth, for the 10x10 cm field, with the 6 MV beam (SSD=100 cm). Table II shows the quantitative statistical results obtained in each region of interest: the first and the second columns indicate the region of interest under study, in the third column we reported the distance between the two distributions (Kolmogorov-Smirnov test statistics) and in the fourth column we listed the corresponding p-value. In any region

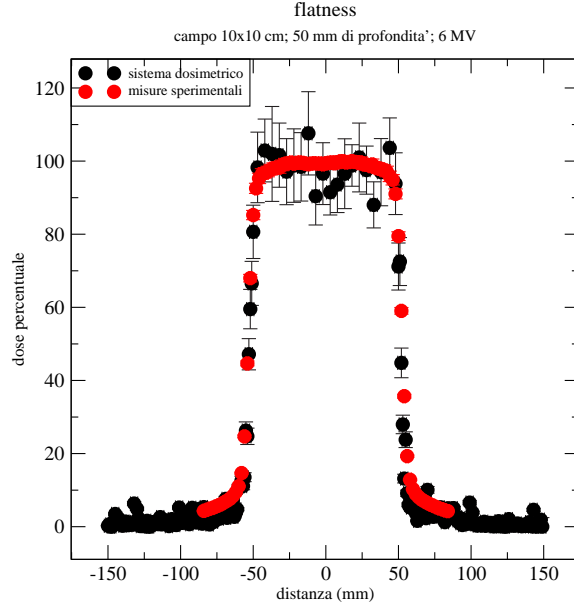


**Figure 1: Lateral dose profiles at 50 mm depth, for the 10x10 cm field, with the 6 MV beam. The red symbols correspond to the experimental measurements, the dark symbols correspond to the Geant4 simulation.**

**Table I: Results of the Kolmogorov-Smirnov test for the lateral dose profiles at of 50 mm depth, for the 10x10 cm field, with the 6 MV beam.**

region of interest	range	distance	p-value
tail	-84, -60 mm	0.39	0.23
high gradient zone	-59, -48 mm	0.27	0.90
central flat zone	-47, 47 mm	0.43	0.19
high gradient zone	48, 59 mm	0.30	0.82
tail	60, 84 mm	0.40	0.10

considered, the Kolmogorov-Smirnov test pointed out a good agreement between experimental data and Geant4 simulations (p-values > 0.05 in any case).

### 3.2 Field 5x5 cm

After the 10x10 cm field, we studied the 5x5 cm field, that have dimensions similar to the fields used in IMRT.

In Figure 3 we show the lateral dose profiles at 15 mm depth, for the 5x5 cm field, with the 6 MV beam (SSD=100 cm).

Table III shows the quantitative statistical results obtained in each region of interest: the first and the second columns indicate the region of interest under study, in the third column we reported the distance between the two distributions (Kolmogorov-Smirnov test statistics) and in

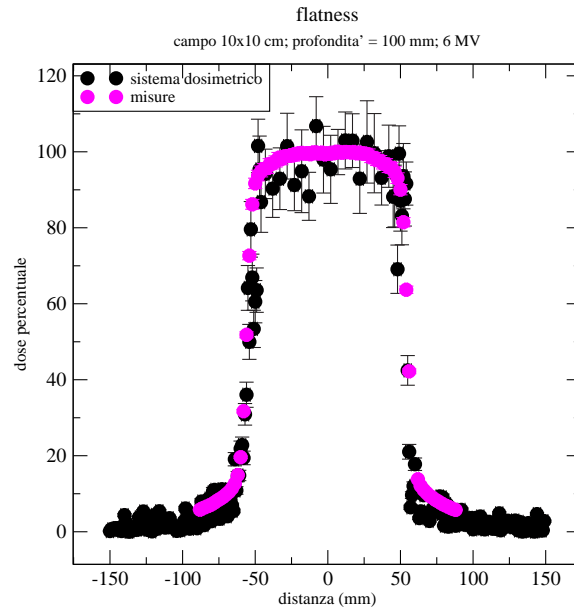


**Figure 2: Lateral dose profiles at 100 mm depth, for the 10x10 cm field, with the 6 MV beam. The pink symbols correspond to the experimental measurements, the dark symbols correspond to the Geant4 simulation.**

**Table II: Results of the Kolmogorov-Smirnov test for the lateral dose profiles at 100 mm depth, for the 10x10 cm field, with the 6 MV beam.**

region of interest	range	distance	p-value
tail	-84, -64 mm	0.43	0.25
high gradient zone	-63, -46 mm	0.33	0.60
central flat zone	-45, 50 mm	0.52	0.17
high gradient zone	51, 56 mm	0.52	0.65
tail	57, 84 mm	0.38	0.40

the fourth column we listed the corresponding p-value. In any region considered, the Kolmogorov-Smirnov test pointed out a good agreement between experimental data and Geant4 simulations (p-values > 0.05 in any case).

In Figure 4 we show the lateral dose profiles at 100 mm depth, for the 5x5 cm field, with the 6 MV beam (SSD=100 cm). Table IV shows the quantitative statistical results obtained in each region of interest: the first and the second columns indicate the region of interest under study, in the third column we reported the distance between the two distributions (Kolmogorov-Smirnov test statistics) and in the fourth column we listed the corresponding p-value. In any region considered, the Kolmogorov-Smirnov test pointed out a good agreement between experimental data and Geant4 simulations (p-values > 0.05 in any case).

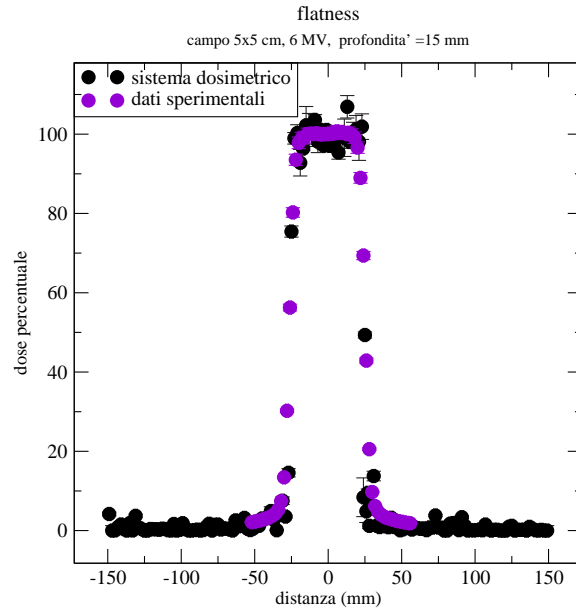


**Figure 3: Lateral dose profiles at 15 mm depth, for the 5x5 cm field, with the 6 MV beam. The violet symbols correspond to the experimental measurements, the dark symbols correspond to the Geant4 simulation.**

**Table III: Results of the Kolmogorov-Smirnov test for the lateral dose profiles at 15 mm depth, for the 5x5 cm field, with the 6 MV beam.**

region of interest	range	distance	p-value
tail	-56, -35 mm	0.26	0.89
high gradient zone	-34, -22 mm	0.43	0.42
central flat zone	-21, 21 mm	0.38	0.08
high gradient zone	22, 32 mm	0.26	0.98
tail	33, 56 mm	0.57	0.13

**Table IV: Results of the Kolmogorov-Smirnov test for the lateral dose profiles at 100 mm depth, for the 5x5 cm field, with the 6 MV beam.**

region of interest	range	distance	p-value
tail	-61, -35 mm	0.33	0.5
high gradient zone	-34, -26 mm	0.40	0.75
central flat zone	-25, 21 mm	0.32	0.24
high gradient zone	22, 32 mm	0.27	0.75
tail	33, 61 mm	0.21	0.91

### 3.3 Field 40x40 cm

We have started to study the 40x40 cm field, that can help us to determine if we have used the correct parameters characterizing the initial electron beam.

In Figure 5 we show the depth dose curves at 100 mm depth, for the 40x40 cm field, with the 6 MV beam (SSD=100 cm). Table V contains the results of the Kolmogorov-Smirnov test, the test demonstrate that the dosimetric system can simulate with great accuracy the experimental measurements.

**Table V: Results of the Kolmogorov-Smirnov test for the depth-dose curves, for the 40x40 cm field, with the 6 MV beam.**

range	distance	p-value
0, 300 mm	0.005	1

### 3.4 Field obtained with intensity modulated beams

We studied an intensity modulated field used to treat a patient with prostate cancer. This field was obtained superimposing two fields shaped with the multileaf collimator, the first field is shown in figure 6; this figure represents the dose distribution in a plane, obtained with the simulation system; the sizes of the symbols in the picture are proportional to the absorbed dose.

Figure 7 shows the whole intensity modulated field; this figure illustrates the dose

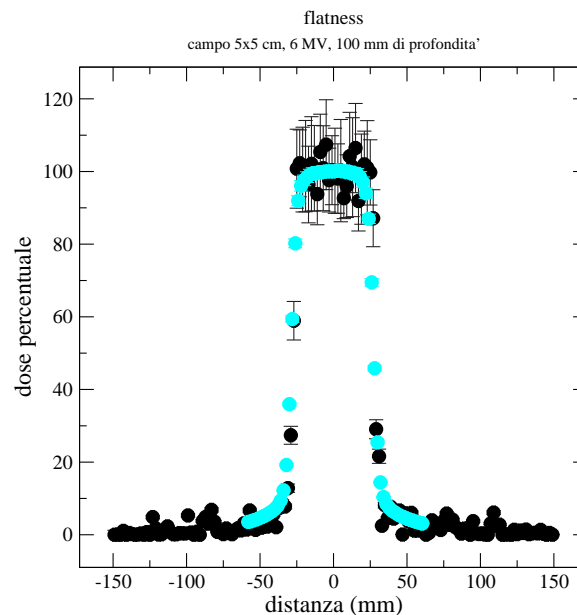


**Figure 4: Lateral dose profiles at 100 mm depth, for the 5x5 cm field, with the 6 MV beam. The azure symbols correspond to the experimental measurements, the dark symbols correspond to the Geant4 simulation.**

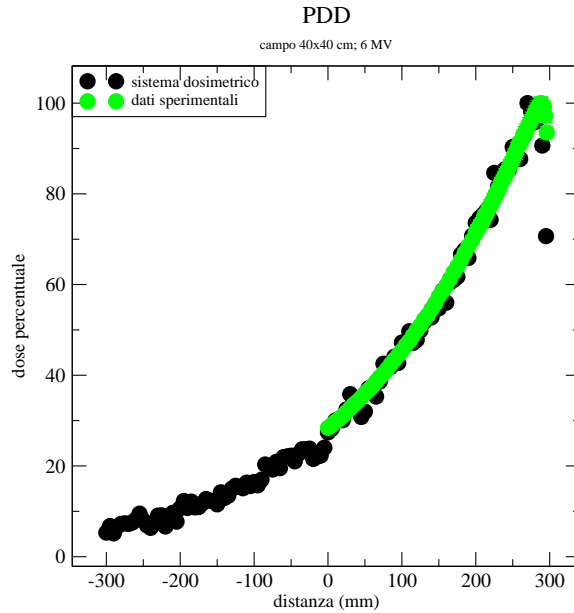


**Figure 5: Depth dose distribution, for the 40x40 cm field, with the 6 MV beam. The green symbols correspond to the experimental measurements, the dark symbols correspond to the Geant4 simulation.**

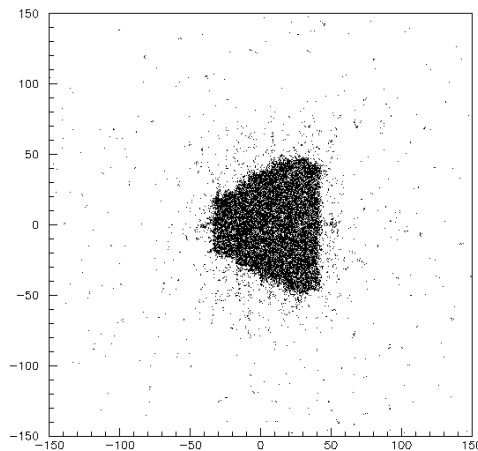


**Figure 6: Dose distribution in a plane given by the modulated beam, this distribution was obtained with the simulation system; the dimensions of the symbols in the picture are proportional to the absorbed dose.**

distribution in a plane, obtained with the simulation system.

In both the figures 7 and 6 we can appreciate the regions with different dose intensity, and we can see that the simulation system is able to reproduce the dose distribution, and in particular the dose interleaf transmission due to the rounded leaf tips.

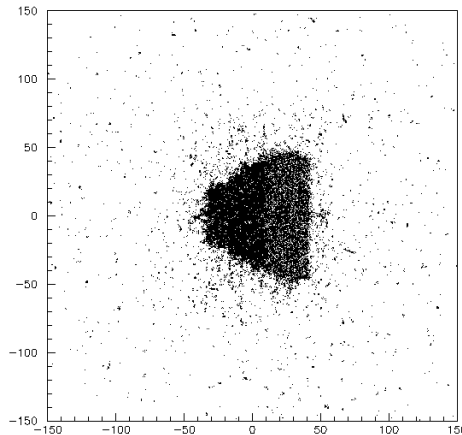


**Figure 7: Dose distribution in a plane given by the modulated beam, this distribution was obtained with the simulation system; the dimensions of the symbols in the picture are proportional to the absorbed dose.**

#### 4 CONCLUSIONS

The results obtained with Geant4 simulation for the fields in homogeneous phantoms show an excellent agreement with the measured dose data. All the statistical comparisons state that there is not a statistical difference between the experimental measurements and the data obtained with the Geant4 simulations.

This method of dose calculation can be a dosimetry tool in addition to the traditional analytical treatment planning systems.

This simulation can be used, changing some parameters in the modelization of the geometry, to study also others medical linac's heads. The linac simulation system tool is publicly available with the public release of Geant4 as an Advanced Example.

#### 5 REFERENCES

1. Geant4 Collaboration, "Geant4 - a simulation toolkit", *NIM A*, **vol. 506**, pp. 250-303 (2003).
2. S. Chauvie, G. Depaola, V. Ivanchenko, F. Longo, P. Nieminen, M.G. Pia, "Geant4 Low Energy Electromagnetic Physics" *Proceedings of CHEP 2001*, Beijing, China, 2001, pp. 337-340 (2001).
3. International Atomic Energy Agency, *Absorbed Dose Determination in External Beam Radiotherapy: An International Code of Practice for Dosimetry Based on Standards of Absorbed Dose to Water*, **Technical Reports Series No. 398**, IAEA, Vienna (2000).
4. G.A.P. Cirrone, S. Donadio, S. Guatelli, A. Mantero, B. Mascialino, S. Parlati M.G. Pia, A. Pfeiffer, A. Ribon, P. Viarengo "A Goodness-of-Fit Statistical Toolkit" *Transactions on Nuclear Science*, **vol. 51 (5)**, pp. 2056-2063 (2004).

5. A.N. Kolmogorov, “Sulla determinazione empirica di una legge di distribuzione”, *Giornale dell’istituto italiano degli attuari*, **vol.4**, pp. 83-91 (1933).